Influence of basalt and hashma industrial waste powder on characteristics of self-compacting concrete

Hagar M. Ali [1,*] **,Mohamed S. Saif** [2]**, Mohamed O.R. El-Hariri** [2]**, Amr Gamal** [2]

[1] *Department of Civil Engineering, PHI- Pyramids Higher Institute for Engineering and Technology, Giza, Egypt.*
[2]*Department of Civil Engineering, Faculty of Engineering at Shoubra, Benha University, Cairo, Egypt*
Corresponding author

E-mail address: h.mohammed17756@feng.bu.edu,eg , mohamed.ismaeel@feng.bu.edu.eg, osama.alhariri@feng.bu.edu.eg, amr.gamaleldin@feng.bu.edu.eg

Abstract: The stone industry generates huge amounts of solid waste powders causing serious several environmental problems. Disposing of these wastes safely requires a large cost. Exploiting and getting rid of them has become essential. This research investigates the impact of incorporating basalt industrial waste powder (BS) as a partial substitute for cement, as well as waste powder from hashma (HM) stone industry as a partial substitute for sand on fresh, mechanical, permeation characteristics of self-compacting concrete (SCC). In addition, the microstructure of the concrete using SEM, XRD and BET has been investigated. Furthermore, environmental and economic studies were conducted. Fresh properties of mixes were measured in terms of slump flow, T50, V-funnel and J-ring tests. To measure mechanical properties of SCC were compressive strength, splitting tensile strength and ultra-sonic pulse velocity were determined. BS was replaced cement by 5, 10, 15 and 20% while HM was replaced sand by 10, 20, 30%. The result showed that BS decreased the fresh properties and use of HM required high dosages of chemical admixture to achieve SCC requirements. Compressive strength improved by incorporating BS with 5% optimum replacement ratio. However, incorporating HM significantly improves compressive strength with increasing replacement ratio. Maximum improved compressive strength reached 17% higher than the control mix (without waste powders) by incorporating 5%BS and 30% HM (mix B5H30). Sorptivity decreased by 20, 21 and 30% while, UPV increased by 9, 13 and 17% for a mix containing 5%BS, 30%HM and (5%BS+30%HM) respectively. This is explained by the reduction in porosity as confirmed by microstructure studies. Incorporating both BS and HM increases the cost of the mix but improved the environmental impact.

keywords: Hashma powder, basalt powder, Self-compacted concrete, mechanical properties, Microstructure.

1. Introduction

The building sector consumes approximately from 35 to 40 percent of raw materials worldwide, resulting in a major consumer of natural resources. Moreover, it emits nearly 35% of the world's carbon dioxide emissions and uses 40% of the world's energy production and 15% of the water supply [1] .The construction industry's sustainable management of natural resources is critical for a more environmentally friendly future, given its considerable impact on the economy and the environment. Both sand and gravel are frequently used as the main raw materials in building, either as fine or coarse aggregate for concrete. These materials are essential to the total volume of concrete. By volume or mass, sand alone utilizes approximately more than one-third of the aggregates [2–3].

As the need for construction continues to rise, the demand and cost of materials used in construction also increase. Concrete, being one of the oldest construction materials, remains a reliable choice in the industry. On the other hand, different minerals can be added to replace some of the cement in concrete, contributing to its more cost-effective and environmentally friendly. This not only reduces the cost of cement but also allows for the production of composite cement using different materials with binding and /or pozzolanic characteristics. Composite cement requires less energy than Portland cement and offers additional improved properties, making it widely used in the building sector. Natural and artificial pozzolans are both frequently used in the creation of composite cement. Volcanic tuffs, volcanic glass, volcanic ash, diatomite, and heat-treated clay are examples of naturally occurring pozzolans [4–6]. Researchers are currently directing their attention towards finding alternative materials for concrete production due to the limited supply of traditional constituents. By replacing these materials, the cost of concrete can be reduced while maintaining its quality standards. Consequently, there is a growing emphasis on discovering new sources of raw materials for concrete. This has resulted in increased research on utilizing various substances as substitutes for fine aggregate or cement, either as fillers or replacements.

Fillers are substances utilized in concrete to occupy spaces between aggregates, thereby reducing the need for binders and enhancing the characteristics of the composite materials when combined with cement. They play a crucial role in enhancing particle arrangement and, most importantly, contribute to the development of additional attributes in newly mixed concrete, according to European EN 13139-2018 [7].

The use of fillers in place of Ordinary Portland Cement (OPC) reduces the amount of cement used, which helps to mitigate the environmental effect of cement production. The use of limestone powder as a filler is common in European

countries. This method improves the initial strength by increasing the duration of cement phase hydration and reducing bleeding, in addition to providing benefits for the environment and economy [8]. Numerous studies investigated how fillers affect certain concrete performance metrics. By increasing density, encouraging hydration through nucleation sites, and interacting with cement components, fillers can affect the physical characteristics of concrete [9]. Soroka and Setter investigated the effects of several fillers with different replacement percentages and fineness levels. Filler-infused mortars showed greater strengths as compared to the control mixture [10]. Non-pozzolanic filler, regardless of its chemical composition, have been shown to primarily accelerate reaction rate, resulting in an increase in early age strength [11].

Fillers are added to concrete to help reduce the size of pores, improve the microstructure and reduce permeability [12]. This, consequently, improves the durability of concrete over time. Studies have shown that adding C-S-H to cement mixes accelerates the hydration process. According to the results, CSH gel, or prehydrated. C_3S seeds, act as a catalyst to hydrate C_3S. According to Thomas et al. [13], adding a small amount of CSH to cement causes a significant change in the primary hydration peak's occurrence, a reduction in the induction period, and an increase in the amount of hydration that occurs in the first few hours. This behavior can be explained by the hydration of cement particles, which creates more sites for nucleation [13]. Hubler et al. [14] have proposed that the reactivity of blended cements can be modified to align with that of Portland cement through the incorporation of seeds within the system. The type of filler significantly impacts the bleeding and segregation resistance of flowable and SCC concrete. This means that the SCC must be in a high flow-ability or fluidity state enabling it to completely filling and smoothly passing through the heavy and congested reinforcement avoiding blocking and segregation. The abovementioned key properties, referred to as "workability", have a marked effect on the strength and durability performance of the hardened SCC [15]. The methodology of selecting the suitable amount of materials and admixtures such as limiting the volume of coarse aggregates, increasing the powder content, superplasticizers (SP), viscosity-modifying agents (VMA), and high paste volume, in addition to the processes of mix design, are essential key parameters for achieving the acceptable self-compactability of concrete mix in its fresh state [16,17]. In the self-compacting concrete sector, the high range of powder content (cement and mineral additives) is one of the guidelines that controlling the fluidity characteristics of concrete mix, therefore facilitating the free vibration - self placing, preventing the coarse aggregate blockage, and improving the microstructure, mechanical and durability performance [18]. Therefore, the majority of the previous studies utilized different by-products such as blast furnace slag, silica fume, fly ash, and limestone wastes as mineral additives separately or in combination with or without ornamental stone wastes in the preparation of SCC mixes [19, 20, 21].

When compared to pozzolanic fillers like metakaolin and silica fume, the use of non-pozzolonic fillers like marble and granite dust reduces bleeding and segregation [22].

Thousands of tons of waste from the processing, grinding, polishing, and hashma industries are being released in Egypt. Shaqa Althueban in east Cairo is the site of a large concentration of hashma and basalt process companies, which are accountable for the annual disposal of hundreds of tons of waste into the environment. This kind of fine material storage presents significant environmental challenges. The development and deleterious dispersion of tiny particles in air, water, and soil are greatly facilitated by dust emitted into the environment [11,23]. Dusts have the identical chemical and mineral composition as the bedrock they come from. This property attributes those to suitable for use in the production of cement mortars and concretes, acting as a partial substitute for cement or fine aggregate. Through doing this, waste management will improve in addition to lowering the cost of construction production. This strategy is in line with the sustainable development goals, which encourages the effective management of non-renewable natural resources and their replacement with waste products that have been recycled. The application of rock dusts from various geological origins as a substitute for cement can aid in mitigating the environmental consequences associated with the growing demand for concrete production. However, it is crucial to have a comprehensive understanding of the impact of such dusts on concrete properties. The inclusion of rock powder significantly affects the characteristics of cement1 composites. Rock dust's influence is mostly due to its filler effect, which is caused by numerous causes, including altered distribution of particle sizes, the development of hydration products (especially CH & CSH) on stone dust particles (heterogeneous nucleation), and cement dilution. These variables, which are dependent on how finely the rock dust is compared to the cement, are important in determining the properties of cement composites (24).

In this study, sand and cement was partially replaced with hashma and basalt dust powder, respectively. Various tests will be conducted to explore the effect of these two materials individually and/or together on SCC concrete, particularly strength and microstructure characteristics.

2. Used Materials

Cementitious materials were ordinary Portland cement (OPC), CEM I-52.5N, conforms to EN 197/1 and silica fume with a specific surface area of 17,500 cm^2/g and spherical particle sizes between 0.1 and 1 μm. Table 1 lists the chemical and physical characteristics of both cement and silica fume. The coarse aggregate used was of crushed dolomite, which satisfies the Egyptian Standard Specification [(E.S.S. No. 1109\ 2008)]. Its specific gravity is 2.70 t/m^3 and a modulus of fineness 6.64. The shape of these particles was irregular and angular with a very low percentage of flat particles. The delivered crushed dolomite size 1 had a maximum nominal size of 9.5 mm.

Natural sand that conforms to ASTM C33 with specific density of 2.60 and a fineness modulus of 2.75 was used as
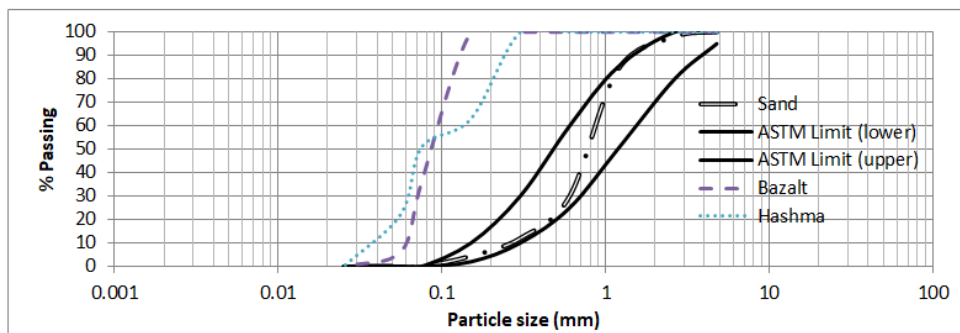
fine aggregate. The particle size distribution of sand and powder is displayed in Figure 1.

Basalt powder was used with a specific surface area of 12,850 cm²/gm as a cement alternative. The utilized basalt powder has a specific gravity of 2.5. The XRD results for the utilized basalt powder pass sieve No. 100 (150 μm) are shown in Figure 2, hashma powder pass sieve No. 80 (180 μm). Mixtures required high range water-reducing admixtures because of the low water-to-binder ratio. To get a suitable consistency of SCC, a polycarboxylates the superplasticizer having a density of 1085 kg/m³ was utilized.

Table1. The physical characteristics and chemical composition of the cementitious and fine materials utilized

Compound (%)	Cement	Silica fume	Basalt	Hashma
SiO_2	21.20	96.0	34.68	9.22
AL_2O_3	5.50	0.10	8.84	0
Fe_2O_3	3.20	1.0	30.07	8.13
CaO	63.4	0.20	12.58	75.22
MgO	0.70	0.15	5.82	3.20
SO_3	2.40	0.10	0.07	0.03
Na_2O	0.10	0.10	1.76	0.9
K_2O	0.50	0.20	1.19	0.13
CL^-	---	----	2.01	1.55
P_2O_5	---	---	0.60	0.23
loss on ignition	3.00	2.15	1.25	1.75
Color Powder	Gray	Light Gray	Dark gray	Gold yellow
Grain Size	90 μm	1 μm	43 μm	33 μm
Specific Gravity	3.15	2.17	2.5	2.08
Bulk Density (t/m³)	1.51	0.355	1.7	1.85

Figure1. Particle size distribution of sand and powder.
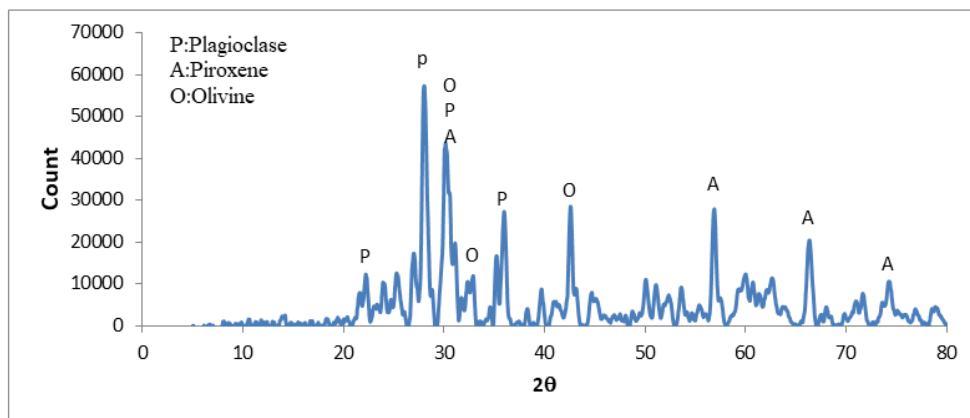
Figure 2. Basalt powder X-ray diffraction patterns.

3. Experimental Study

The processes of batching, mixing, and casting were carried out with careful consideration. First, the fine and coarse aggregates were weighed precisely to within 0.5 grams. A drum mixer was used to prepare the concrete mixture. The fine, coarse, and cement aggregates were mixed well. Water was gradually added after they had been blended to a homogeneous color to ensure that no water was lost. SCC was used to fill the molds. The specimen's upper surface was polished and leveled. The specimens were demolded after a day and placed in a curing tank, where they were left to cure for 7,&28,&56,&90 days.Twenty SCC mixes were adopted using waste material industrial basalt powder (BS) and hashma powder (HM). Mixes were sorted into six groups.

The first Group includes the control mix without BS and HM and four mixes incorporated varying amounts of BS(5%,10%,15% & 20%) as partial cement substitute and 2nd group include three mixes incorporating varying amounts of HM (10%, 20%, and 30%) as partial sand substitute. The remaining groups contain a blend of BS with various percentages (5%, 10%, 15% and 20%) as partial cement substitutes and different percentages of HM (10%, 20% and 30%) as sand replacements. All mixes incorporated 15% silica fume (SF) as partial cement replacement, water to binder ratio was kept constant at 0.39 for all mixes as shown in Table 2.

Every concrete mix was mechanically mixed with a 10 L capacity to ensure homogeneity and reduce particle agglomeration. After mixing all powder ingredients for ten minutes, water and HRWRA were added. Half of the HRWRA diluted in half of the mixing water was gradually added over five minutes period. After mixing for five more minutes, the remaining water and HRWRA were gradually added. Lastly, research was done on the fresh, hardened, and durability properties of SCC mixes, as seen in Figure 3.

Table 2. Concrete mixture ingredients (kg/m3).

	Mix	C	SF	BS	HM	Coarse Agg.	Sand	W	Admix
	B0	467.5	82.5	0	0	940	700	217	4.4
	B5	440	82.5	27.5	0	940	700	217	4.4
G1	B10	412.5	82.5	55	0	940	700	217	4.4
	B15	385	82.5	82.5	0	940	700	217	4.4
	B20	357.5	82.5	110	0	940	700	217	4.4
	B0/H10	467.5	82.5	0	70	940	630	216	4.4
G2	B0/H20	467.5	82.5	0	140	940	560	215	6.4
	B0/H30	467.5	82.5	0	210	940	490	214	7.5
	B5/H10	440	82.5	27.5	70	940	630	216	6
G3	B5/H20	440	82.5	27.5	140	940	560	215	7.5
	B5/H30	440	82.5	27.5	210	940	490	214	8.5
	B10/H10	412.5	82.5	55	70	940	630	216	6.4
G4	B10/H20	412.5	82.5	55	140	940	560	215	7.5
	B10/H30	412.5	82.5	55	210	940	490	214	9
	B15/H10	385	82.5	82.5	70	940	630	216	6.5
G5	B15/H20	385	82.5	82.5	140	940	560	215	8
	B15/H30	385	82.5	82.5	210	940	490	214	9.5
	B20/H10	357.5	82.5	110	70	940	630	216	7
G6	B20/H20	357.5	82.5	110	140	940	560	215	8.4
	B20/H30	357.5	82.5	110	210	940	490	214	9.8
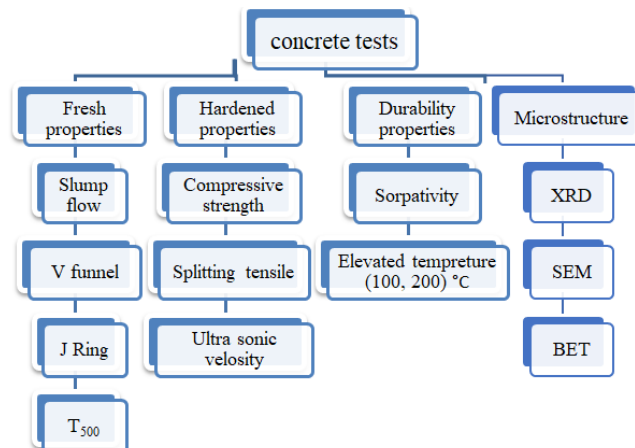
Figure 3. Investigated Fresh& hardened& durability and microstructure characteristics.

3.1 Experimental Tests

3.1.1 Fresh tests

The purpose of the slump flow test was to evaluate the mixes' flowability in the absence of any obstructions. A standard slump cone was used for the test, and the concrete was carefully and compaction-free put into the cone. The slump flow value is determined by elevating the standard slump cone and measuring the average diameter of the concrete.The J-ring test was performed using EN 12350-12. Approximately 7 liters of uncompacted concrete were placed within the cone. When the mold was raised vertically and the concrete stopped flowing, the heights between the surface of the concrete and the top of the J-ring both within and outside the ring in two directions at right angles were measured. The final result, the J-ring blocking step BJ (also called the step height), was calculated using equation (1).

$$BJ\ (m1m) = \frac{\Delta hx1 + \Delta hx2 + \Delta hy1 + \Delta hy2}{4} - \Delta h0 \qquad (1)$$

B_J : J-ring blocking step BJ (also known as the step height), $\Delta h0$: is the height measurement at the center of flow. $\Delta hx1$, $\Delta hx2$, $\Delta hy1$, $\Delta hy2$ are the four measurement heights at positions just outside the J-ring.

The V-funnel was set up according to EN12350-9. The V-funnel test flow time is somewhat correlated with plastic viscosity. It measures how long it takes for a specific volume of concrete to pass through a narrow opening. This test indicates how well concrete fill a space as long as there is no reduction in flowability or blocking.

3.1.2 Hardened and durability tests

3.1.2.1 Splitting and compressive strength test

A 2000 kN compressive testing machine was used for the both splitting and compressive strength tests. The specimens for the compressive test were 100 mm length cubic shapes, whereas the specimens for the splitting test were 100 mm diameter and 200 mm height cylinders. Using standard curing at 20°C, tests were conducted to determine the compressive strength of concrete at various ages, including 7, 28, 56 & 91 days. But the splitting strength test was run at ages 28 and 90 days only.

3.1.2.2 Water absorption by capillary action (Sorptivity)

When concrete or mortar specimen is subjected to water, some water can be absorbed. The amount of water absorbed by capillary action through a specified area of the tested specimen at certain periods can be determined by calculating the difference in weight of the specimen before and after exposure to water (25).

The objective of this test was to measure the rate at which water permeates the concrete's surface. Until the samples attained a constant weight, they were dried at 105°C in an oven. They were put on a support device at the bottom of the pan with a water level of 2 mm just above the top of the support device. Finally the sorptivity of the test specimens was calculated using equation (2) (25). The

results were an average of triplicate specimens tested at the ages of 28 & 90 days.

$$\frac{W}{\rho A} = S\sqrt{t} + I_0 \ldots \ldots \ldots \ldots \qquad (2)$$

Where, W= mass gain (Kg), A = surface area tested (m^2), t= time elapsed (min), at which the weight is determined, S = sorptivity (early age sorption coefficient) in $mm/min^{1/2}$ if 1 min < t < 7 h , I_0 = initial sorption(mm) occurring immediately upon contact with water, ρ= density of water (Kg/m^3)

3.1.2.3 Effect of elevated temperature

In this research, the influence of high temperature (100°C and 200°C) utilizing an electric furnace on the performance of all studied SCC mixtures was examined. For all temperature levels, the samples were subjected to an elevated temperature for 30 minutes at a rate of 3 C per minute. Microstructural analysis was performed on samples that were subjected to 100°C and 200°C temperature.

3.1.2.4 Microstructural analysis

X-ray diffraction (XRD)

(XRD) utilizing a Philips PW/1710 equipment with monochromatic Cu-K 1radiation (λ = 1.54056 Å) at 40KV, 30MA, & a scanning speed of 0.020/sec for a 2 range from 10 to 500.The output from the spectrometer is a trace of intensity (I) against the Bragg angle (Θ), the spacing of the reflecting planes (d) can be computed using The Bragg formula.

$$n\lambda = 2d \sin\theta \ldots\ldots\ldots . \qquad (3)$$

where λ is the radiation wavelength and n is the order of reflection (λ = 1.542 Aº with Cu-K α radiation).

With spacing (d) and intensity (I), the identification of the crystalline compounds can be obtained by comparing with standard data.

Surface area and pore size

The Quanta Chrome Co.'s Nova Touch LX2 surface area and pore size analyzer model was used for the test. Zeta potential and sizing were also determined in this sector by Nano Sight NS500 manufacture by Malven, UK. The pore structure of concrete influences important performance aspects like strength, permeability and durability. Nitrogen sorption techniques based on the Brunauer-Emmett-Teller (BET) principle provide detailed quantification of specific surface area as well as pore volume and pore size distribution through analysis of multilayer adsorption-desorption isotherms.

Scanning electron microscope

SEM allows for nanometer-scale characterization of morphological and compositional aspects in cement and concrete by scanning the sample surface with a focused electron beam and detecting signals generated from beam-sample interactions. SEM imaging provides insights on material phases, defects, and interfacial transition zones. Small concrete fragments was extracted from samples and vacuum impregnated with a low-viscosity epoxy to preserve the structure. After being carefully cut, cured surface mounts was polished in stages using SiC sheets and diamond

suspensions until a 0.25 μm finish is achieved. Then, a small layer of gold-conductive paint was applied. The type Philips XL 30, a scanning electron microscope (SEM) with a voltage of acceleration of 30 KV, magnitude ranges to 400,000X, and sharpness of 3.5 nm was employed.

4.　Results and Discussions

4.1　Fresh Properties

The fresh properties of the SCC mixtures were determined in terms of slump flow, T500, V-funnel and J-ring tests, the results of which are given in Table 3 and indicate a change in workability with the increase in the dosage of superplasticizer to maintain a consistent range of SCC properties according to the EFNARC standards [26].

It was found that the addition of BS decreased slump flow. Similarly, adding HM reduced slump flow, requiring a higher dose of SP to keep up the desired slump flow. In general, the SCC mixtures were observed to be within the limit values given in EFNARC. The slump flow test results varied between 547 mm and 740 mm. The best slump value was achieved by the B20/H10 mixture at 740 mm,

corresponding to a 35% higher flowability than the control mix, as shown in Figure 4.

J- Ring test denotes the passing ability of the SCC. All the mixes satisfy the EFNARC recommendations. To assess flowability and stability of SCC, V-funnel test was conducted. As per EFNARC guidelines [26], the time ranges between 7 to 13 seconds is sufficient to achieve self compactability. According to the test results, the B15/H10 and B15/H20 mixtures had the highest viscosity value among the SSC mixtures containing both wastes powder (basalt and hashma powder).

According to the test results, the more using a lot of powders, the lowest viscosity value among the SSC mixtures. Numerous authors have also reported similar findings regarding SF [27, 28]. A similar response was observed for the ternary and quaternary mixtures following changes to the BS & HM. Increased demand for superplastiezer and lower flowability were caused by materials with rough surface textures, irregular shapes, and higher specific surface areas (measured by Blaine air fineness) (S.F, BS, and HM). [29].
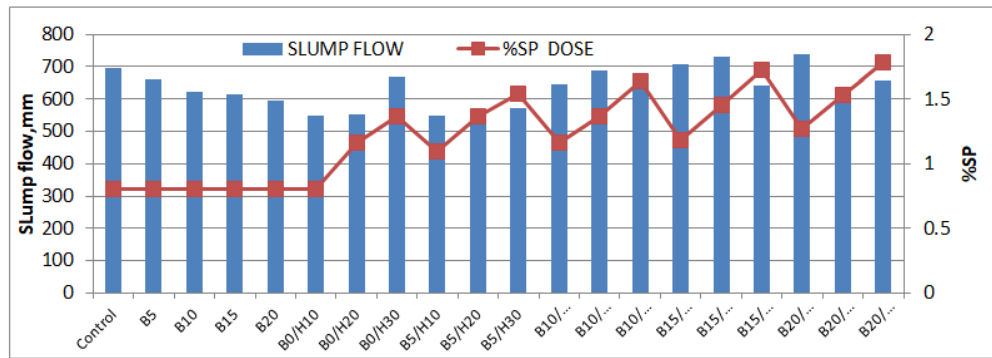

Figure 4. Variation in slump flow and SP dose

Table 3. Fresh properties of mixes.

| Mix ID	Slump Flow (mm)	T_{500} (sec)	V-Funnel (sec)	J-ring BJ(mm)
Control	695	2.60	7	5
B5	660	2.60	7	6
B10	623	3.00	8	7
B15	615	3.00	9	7
B20	595	3.40	9	8
B0/H10	550	4.00	12.5	9
B0/H20	553	4.00	12	9
B0/H30	667	3.60	8	8
B5/H10	547	5.00	13	10
B5/H20	560	4.60	12	9
B5/H30	570	4.00	12	9
B10/H10	647	4.00	9	8
B10/H20	687	3.70	8	7
B10/H30	640	4.00	9	8
B15/H10	707	2.50	7	6
B15/H20	732	2.50	7	6
B15/H30	642	4.00	9	8
B20/H10	740	2.50	7	6
B20/H20	627	4.00	8	8
B20/H30	657	3.50	8	9

4.2 Hardened Properties

4.2.1   Compressive strength

Figure 5 shows the compressive strength values of all studied concrete mixtures tested at different ages (7, 28, 56, and 90 days) under standard water curing. From Figure 5a it can be seen that the two mixtures containing 5% and 10% BS produced higher compressive strength values than the control mix, with the ideal replacement ratio of 5% BS (Mix (B5)). The samples containing 5% and 10% BS showed compressive strength values of 707 and 695 kg/cm^2 at 90 days, respectively, while the control mix's compressive strength at 90 days was 657 kg/cm^2 . For BS replacement ratios more than 10%, the compressive strength decreased compared to the control mix. Notably, it can be concluded that higher BS content limits the compressive strength gain since it lowers the amounts of chemical components (C_3S and C_2S) in the cementitious material, which have an impact on the strength of the concrete. Khodabakhshian et al. [30] reached to similar conclusions. The compressive strength values of concrete mixtures containing varying percentages of HM at different ages are displayed in Figure 5a. At all

testing ages (7, 28, 56, and 90 days), concrete mixtures containing Hashma powder (HM), particularly mix (B0/H30), produced higher compressive strength values than the control mix (B0). In comparison to the control mix, the percentage of compressive strength improvement for mixes (B0/H10), (B0/H20), and (B0/H30) was 4%, 7%, and 8%, respectively.

Figure 5b, shows the compressive strength values for mixes incorporating both 5% BS and different percentage of HM (10, 20 and 30%). This figure illustrates how compressive strength increases with increasing HM content. Compressive strength values were 709, 722 and 765 kg/cm^2 for B5/H10, B5/H20 and B5/H30 mix respectively for 90 day curing period. The remarkable compressive strength improvement achieved for mixture B5/H30 was 16.5% higher than the control mix (657 kg/cm^2). Moreover, the same figure shows higher compressive strength with incorporating 10% BS and different content, of HM (10, 20 and 30%). However, the improvement level was lower than mixes containing 5% BS. The percent of improvement was 12% for B10/H30 compared to the control mix.
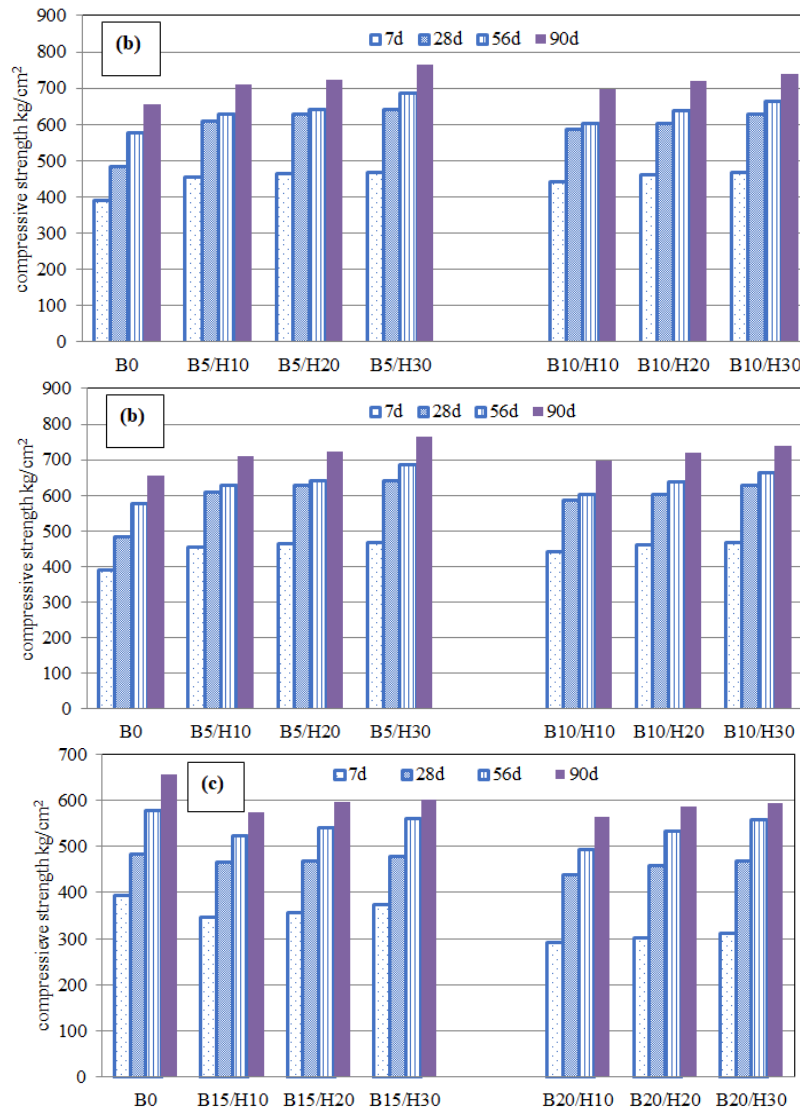
Figure 5. Compressive strengths for all mixes at 7, 28, 56, and 90 days

Figure 5c, shows a reduction in compressive strength with increasing BS content beyond 10% for blended mixes and degradation in compressive strength increases with increasing BS content while decreases with increasing HM content. The maximum percent of reduction was 13% and 15% for B15/H10 and B20/H10 mixes, while the minimum reduction was 8% and 10% for B15H30 and B20H30 mixes respectively compared with the control mix.

The physical effect of HM, also known as the filler effect, may be responsible for the additive's positive impact on the mechanical properties of concrete. The voids (pores) between the sand grains and coarse aggregate are filled with HM granules. Higher aggregate fineness and a more compact cement matrix microstructure lead to decreased porosity and increased compressive strength [31, 32]. The grain size distribution curve of BS, and HM are shown in Figure 1. These tiny particles were probably packed among somewhat larger cement grains, which sealed the cement matrix's microstructure and enhanced the mechanical characteristics of mortars & concretes. The addition of BS has raised the amount of active centers particularly the C-S-H phase, which also affects the increased strength of the concrete where hydration products can crystallize. Because cement granules have differing electrostatic charges, they prefer to attract each other in water slurry, which causes flocculation, or the formation of aggregate. In this instance, not all of the cement particles are efficiently utilized in the hydration process, and water is unable to readily permeate all of the spaces between the cement grains. The introduction of micro filler results in increased cement grain dispersion, which speeds up the hydration of clinker phases and, ultimately, the increase in strength [32, 33].

4.2.2 Splitting tensile strength

The specimens' Splitting Tensile Strength (STS) values at 28 and 90 days are displayed in Fig. 6. The trend of STS and compressive strength are similar. The tensile strength values of mixes containing HM are higher than that mixes containing BS. Mixes containing 5% and 10% BS improved STS by 11% and 5% respectively compared with the control mix while mixes containing 15% and 20% BS show reduction in STS by 5% and 8% respectively compared to control mix. The effect of incorporating HM seems different, STS increases with increasing HM content. STS increased by 9%, 21% and 33% for 10, 20 and 20% HM addition respectively compared to control mix B0. Inclusion of both BS and HM together improved STS compared with control mix. On the other hand, the level of improvement increased with increasing HM content and decreased with increasing BS from 5% to 10%. The percent's of improvement in STS were 12%, 28%, 37%, 12%, 21%, 27% for mixes B5/H10, B5/H20, B5/H30, B10/H10, B10/H20 and B10/H30 compared to control mix respectively. The optimum improvement in STS achieved in B5/H30 mix however, mix B10/H30 contain a higher percent of waste powder which could imposes better environmental and economic impact (eco-friendly). On the other hand, higher percents of BS (15 and 20%) incorporation in blended mixes cause a reduction in STS than control mix. The percent of reduction increases with increasing BS and decreases with increasing HM contents.

4.2.3 Ultrasonic pulse velocity

The non-destructive Ultrasonic Pulse Velocity (UPV) test was used to evaluate the quality of concrete. By using electronic wave transfer, this test also provides insight into the different types of faults found inside concrete [34]. The likely reasons for the observed decreases in UPV values are non-homogeneity, weak particle packing, pores, and other defects [33]. In general, UPV values increase as HM content increases as shown in Fig.7. It is worthy mention that UPV is dependent on both the concrete density and the volume of voids. UPV follows the same trend as that of compressive strength and STS. The velocity range of UPV is 4.85 - 6.1 km/s. This variation is explained by the percentage of internal voids and the densification degree of the structure. It was found that B5/H30 mix shows the highest UPV value of 6.1 Km/s which represent 16.7% improvement compared to the control mix (5.4 Km/s).
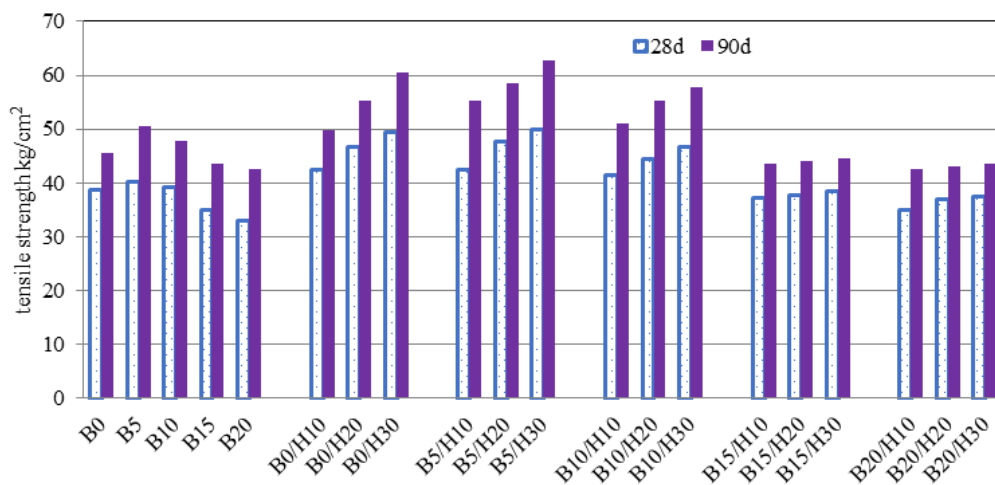

Figure 6. Splitting tensile strength after 28 and 90 days for all mixes

4.3 Durability Properties

4.3.1 Sorptivity

Capillary suction, which is mostly governed by the number and continuity of capillary pores, is the essential feature that allows the concrete sample to absorb water. Consequently, the concrete specimen's mass increases and is monitored over time, enabling the determination of its sorptivity. The sorptivity test results, which ranged from 8.14 to 5.11 mm/min$^{1/2}$, are displayed for all mixes in Figure 8. With 5.11 mm/min$^{1/2}$, the B5/H30 mix's sorptivity value was 30% lower than that of the control mix. The inclusion of SF to decreases the pores due to its high pozzolanic activity and its micro filler effect, thus, it plugs the pores in addition to the small size HM particles.

4.3.2 Effect of elevated temperature

The microstructure of concrete is dense, and when it is exposed to high temperatures, it may be more prone to explosive spalling. All specimens were subjected to high temperature (between 100 and 200°C) in order to investigate the effects of elevated temperatures. After the concrete was exposed to high temperatures (100°C and 200°C), its compressive strength was measured. The results were compared to companion samples that were cured at a standard temperature of 22°C. According to the results, the compressive strength increased as the moisture content dropped at high temperature. It was observed that the compressive strength increases for mixes from 22°C to 200°C. Figure 9 displays the percentages of compressive strength increase at elevated temperature (100°C and 200°C) for all studied mixes. At 100 °C and 200 °C, respectively, the percentage of increase in compressive strength ranged from (0.26% and 2.37%) to (0.41% and 2.13%), the percentage of increasing compressive strength was less than 3%. Behnood and Ziari [35] noticed that the compressive strengths little rose for mixtures containing silica fume at 200 °C and more increasing at up to 200 °C.
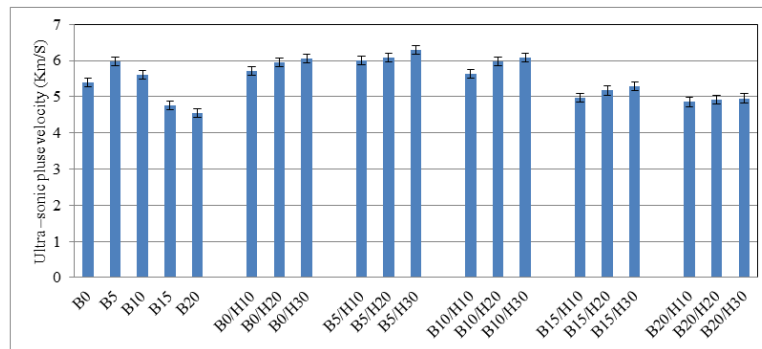

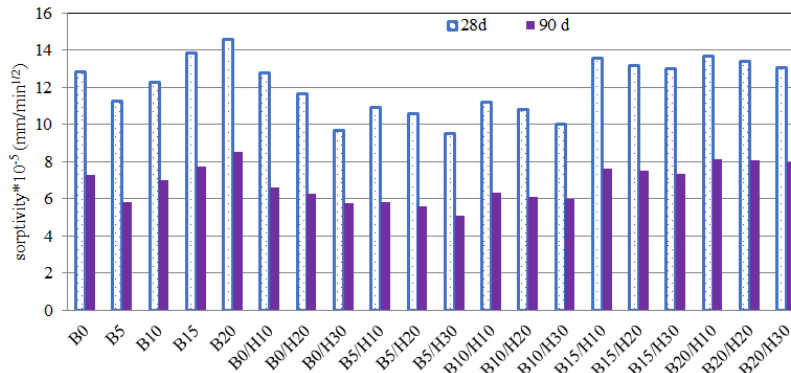**Figure 7.** Ultrasonic pulse velocity for all studied mixes at 90 days

Figure 8. Sorptivity for all studied mixes at 28 and 90 days.
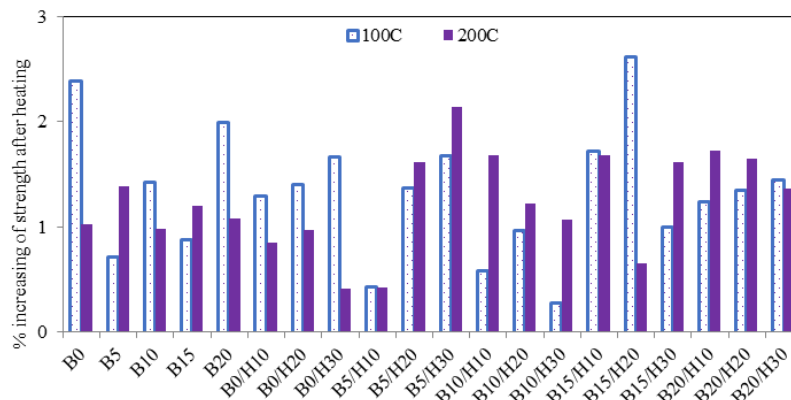

Figure 9. Compressive strength values at elevated temperatures

4.4 Microstructure Analysis

XRD, SEM, and BET were used to examine both the microstructure and the morphology in control mix B0, B5, B0/H30, and B5/H30, at 28 days .

4.4.1 XRD analysis

Fig.10 (a0, b0, c and d) demonstrate XRD diffraction pattern of four chosen specimens. The main hydration product identified was calcium0 silicate0 hydrate (C-S-H), seen for a broad hump centered at 30-35° 2θ in all tasted samples. Portlandite peaks at 18.0°, 34.1°, 47.1°, 50.8° and 54.3° 2θ were sharp and distinct in most samples, indicating abundant calcium hydroxide formation. Secondary reactions were also observed - the presence of ettringite peaks at 9.0°, 15.7°, 25.1° 2θ in some samples pointed to additional aluminate reactivity. Calcite peaks at 29.4°, 36.0°, 39.2° and 47.5° 2θ were seen in a few matured concrete samples as well. Rietveld refinement of the XRD data allowed quantification of the phase abundances. The relative percentages of key phases same calcium0 silicate0 hydrate (C-S-H), portlandite, calcite & ettringite were estimated in each sample. Fig (9-a) (B0) shows the presence of $Ca(OH)_2$ crystals indicateing incomplete pozzolanic reaction. This implies unreacted calcium hydroxide, potentially leading to lower strength and durability due to its susceptibility to carbonation, Tricalcium silicate (Ca_3SiO_2) presence signifies residual anhydrous cement clinker, further suggesting limited pozzolanic activity. On other hand Fig 9 (b, c, d) (B5, B0/H30 and B5/H30) displays the absence of $Ca(OH)_2$ peaks suggesting a complete or near-complete pozzolanic reaction. This implies efficient consumption of calcium hydroxide via its participation in pozzolanic reactions, likely contributing to enhanced strength and durability. Presence of

various C-S-H (calcium silicate hydrate) minerals, including ilvaite, jaffeite, ettringite, and prehnite, confirms active pozzolanic reactions. These minerals result from the raction of calcium hydroxide (CH) from the cement hydration with various elements like Si, Fe, and Al present in the pozzolanic additive. Sharp and strong peaks of specific C-S-H minerals, particularly C-S-A-F-H (calcium silico aluminate ferrite hydrate), indicate well-crystallized and potentially denser reaction products. This could further contribute to improved mechanical properties. The XRD results suggest a significantly higher degree of pozzolanic activity in B5 and B5/H30 compared to B0. This is evident from the complete/near-complete consumption of $Ca0(OH)_2$ and the creation of diverse C-S-H minerals. The existence of specific C-S-H minerals like ilvaite and C-S-A-F-H in B5, B0/ H30, and B5/H30 implies a more complex and potentially more effective pozzolanic reaction compared to B0, which primarily exhibits unreacted $Ca,(OH)_2$ and anhydrous clinker. Greater proportion of minerals with C-S-H in B5, B0/H30, and B5/H30 compared to B0 suggests a denser and potentially stronger microstructure, contributing to their superior mechanical properties.

Magdalena Dobiszewska, and Ahmet Beycioglu [31] concluded that very fine particles of dust powder acted as crystallization centers and provided additional areas where C–S–H nuclei can settle. It was observed that the dust powder well adhered to the hydrated cement paste, and the portlandite crystals did not appear in large quantities between the dust and the C–S–H gels. Contrary to reference mixes (without dust powder), this observation indicates that dust powder-substituted concretes have lower porosity through the interfacial transition zone [31].
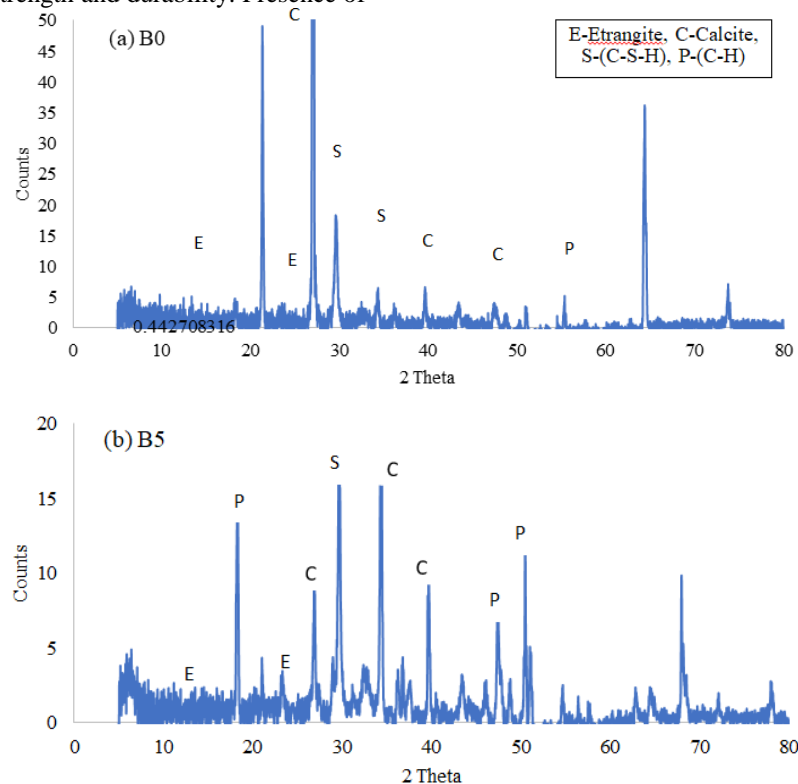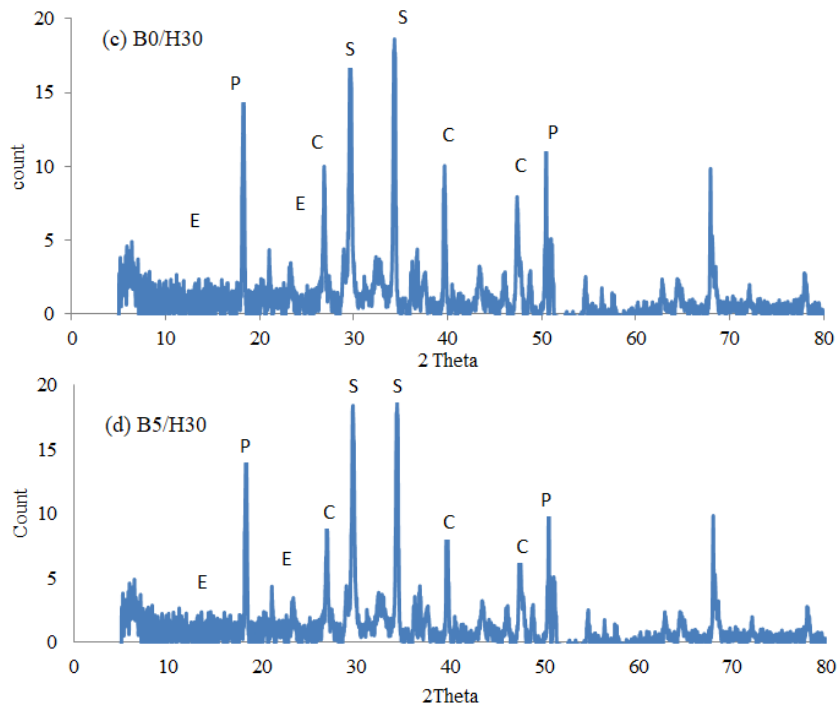
Fig. 10. XRD pattern of four chosen samples (B0, B5, B0/H30 and B5/H30)

4.4.2   SEM analysis

SEM allows for nanometer-scale characterization of morphological and compositional aspects of cement and concrete by scanning the sample surface with a focused electron beam and detecting signals generated from beam-sample interactions. SEM imaging provides insights on material phases, defects, and interfacial transition zones. Control mix B0 shows largely porous, flawed hydration product morphology with very little, long fibers present. In contrast, in the B5, B0/H30 and B5/H30 microstructure, a reduction in flaws and pores is clearly visible. Instead, a dense, compact hydration product matrix with good integration of supplementary reinforcement fibers is seen. Image analysis quantifies these traits - the porosity reduced from 8% in B5 to 3% in B5/H30. The hydration efficiency improved with unhydrated cement reduction from 5% to 0.5%. Meanwhile, the fiber fraction enhanced drastically from 0.2% to 5% volumetrically. Thus, the supplemented blends demonstrate superior particle packing and pozzolanic hydration. This refines pores, provides continuity through the C-S-H and additionally incorporates rigid reinforcing fibers. These synergistic microstructural optimizations rationalize the obvious increase in both compressive strength and STS values measured for sample B5/H30 versus control mix B0 as shown in Figure 11.

4.4.3   Sur0face are0a and po0re si0ze

The analysis of the nitrogen adsorption-desorption isotherms offered insight into the pore properties of the various concrete formulations under examination. Comparison among the reference matrix (B0) and the modified specimens (B5, B0/H30, and B5/H30) revealed noteworthy alterations in the pore structure parameters that were derived from the corresponding isotherms. The reference mix, B0, exhibited an average pore diameter of approximately 245 nanometers. In contrast, the supplementary cementitious materials incorporated into the B5, B0/H30, and B5/H30 blends appeared to refine the pore structure, as evidenced by reducing average pore diameters to 234 nm, 221 nm, and 198 nm, respectively. This trend indicates a progressive diminution in the pore sizes, which suggests that the additives likely contributed for denser 0microstructure & potentially augmented the improvement of mechanical properties. In parallel, the pore surface area measurements, determined by Brunauer Emmet teller (BET) method, disclosed a decrease in pore surface area for the modified concrete mixes relative to the control mix B0, which presented a value of 16.2 square meters per gram. Specifically, the specific surface areas for B5, B0/H30, and B5/H30 were found to be 15.1 m²/g, 14.7 m²/g, and 13.5 m²/g, respectively. These results oppose the anticipated inverse relationship between pore size and specific surface area. In the same time another typical scenario would predict an increase in pore surface area alongside a reduction in pore volume. However, the observed decrement in the specific surface area concurrent with the reduction in average pore diameter implies that other factors may influence the matrix, such as the possible blockage of smaller pores or changes in the pore distribution, potentially induced by the introduction of supplementary materials. This comprehensive analysis of the pore structure after incorporation of additives suggests a more refined and denser matrix, which could be advantageous for durability and compressive strength. Further investigation into the specific nature of the additives and their influence on the hydration process and the resulting microstructure could provide additional insights into the mechanism behind these modifications in the pore characteristics.
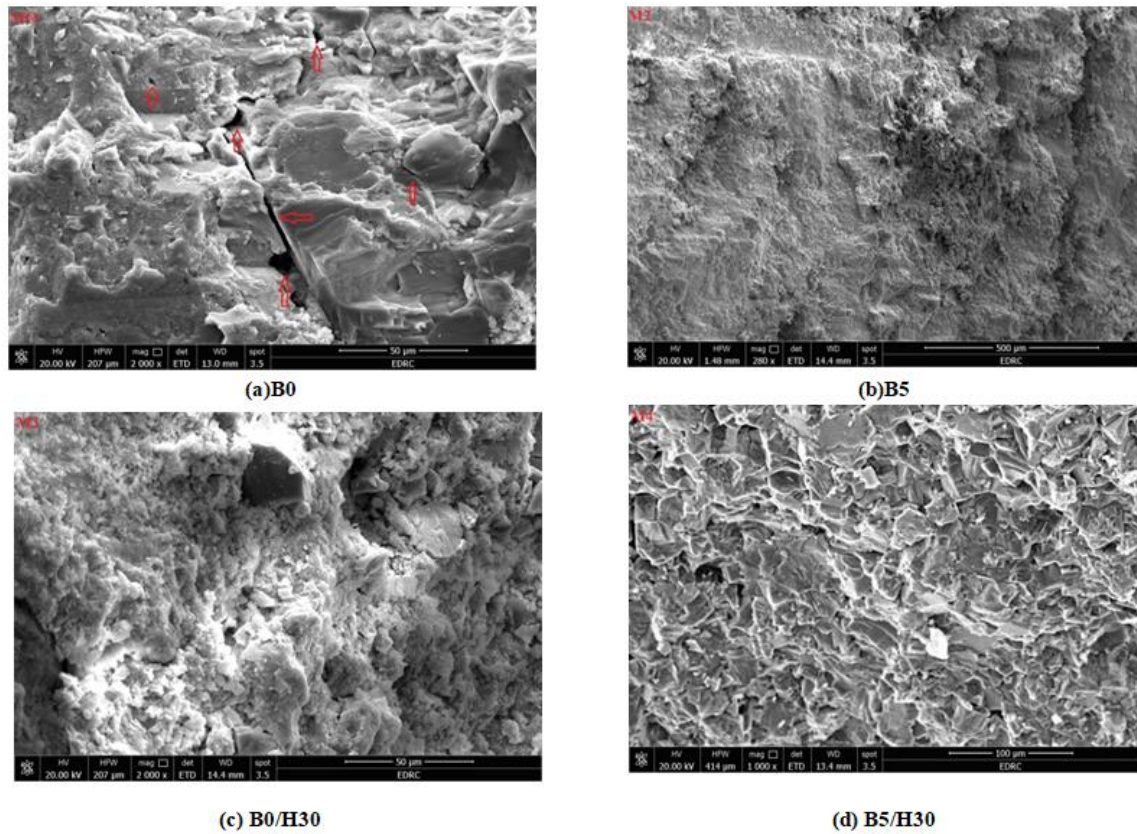
Figure 11. SEM image for mixes B0, B5, B0/ H30 and B5/H30

5. Environmental Study

The direct release of waste into the environment creates environmental problems. Therefore, emphasis has been placed on recycling the waste products from various industries. Wastes can be recycled or used as mixtures to maximize the use of natural resources and save environmental waste. These industrial wastes on neighbouring land depletes the soil of its natural fertility and makes the area look unclean.

Recycled, waste materials and by-products from various industries are used in the manufacturing process of environmentally friendly concrete, which consumes less energy during production. It emits less carbon dioxide, cheaper price and more resilient than conventional concrete. One of the ideal methods for producing environmentally friendly building materials is to partially replace energy-intensive cement with recycled and / or waste materials. Roughly 14 billion cubic meters of concrete are cast annually, according to the Global Cement and Concrete Association (GCCA). Up to 7% of all CO_2 emissions come from the manufacture of cement alone, which is three times more than emissions from aviation. Table 4 shows that the CO_2 emission for producing one ton of cement is 0.83 tons.

As a result, waste materials like basalt powder are used as partial substitution of cement to reduce CO_2 emissions. Normal concrete, also known as conventional concrete, is made composed of superplasticizer, potable water, fine and coarse aggregate and regular Portland cement. Mix 1's CO_2 emissions are 456.5 kg. In order to lower CO_2 emissions a portion of the cement content was substituted with basalt powder and silica fume. With 15% SF and 85% cement in Mix 2 (B0), the CO_2 emission was 388.025 kg. Mix 3(B5) had 15% SF, 5% BS, and 80% cement; the amount of CO_2 released was 365.2 kg. With 15% SF, 10% BS, and 75% cement in Mix 4 (B10), the CO_2 emission was 342.375 kg. Fig.12 shows CO_2 emissions per concrete cubic meter for various mixtures.

6. Economic Feasibility of the Study

The costs associated with the production of one cubic meter from all studied mixtures are shown in Table 5 and Fig. 13. Evidently, as the level of basalt powder inclusion increased, the cost of the concrete mixes decreased. For instance, the cost of the control mix was reduced from EGP 2015 to EGP 1969.625 and EGP 1924.25 when 5% and 15% of OPC were replaced with BS, respectively. The cost savings was due to using waste basalt powder instead of OPC. On contrary the total cost of concrete containing hashma powder increased in comparison with control mix. This is due to the cost of increasing amounts of superplasticizer needed for mixes containing hashma to maintain the same level of flowability. Among all studied concrete mixtures, mix B5 and mix B10 achieved the best cost saving and improvement in concrete properties. Although partial replacement of sand with hashma powder resulted in an obvious improvement in concrete properties, it was noticed the increase in cost was about 11% and 18% for B0/H20 and B0/H30, respectively, compared to control mix as shown in Table 5 and Figure 13.

**Table 4.** Carbon that is embodied from cement manufacture.

Material	Embodied carbon (KgCO$_{2e}$/Kg)	Referance
Portland cement	0.83	Hammond andJones, 2008)(36)
	0.83	(Chiaia et al.,2014)(37)
	0.82	(Reiner, 2007)(38)
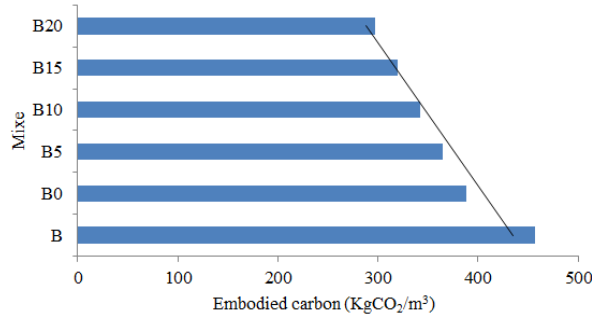
Figure 12. CO2 emissions for different mixes.

Table 5. Cost per cubic meter in Egyptian pounds of studied mixtures (year 2021 prices)

Mix	C	BS	SF	Coarse Agg.	Sand	Admix	HM	Cost/m^3
B0	794.75	0	539.55	112.8	39.9	528	0	2015
B5	748	1.375	539.55	112.8	39.9	528	0	1969.625
B10	701.25	2.75	539.55	112.8	39.9	528	0	1924.25
B15	654.5	4.125	539.55	112.8	39.9	528	0	1878.875
B20	606.9	5.5	539.55	112.8	39.9	528	0	1832.65
B0/H10	794.75	0	539.55	112.8	35.91	528	3.5	2014.51
B0/H20	794.75	0	539.55	112.8	31.92	768	7	2254.02
B0/H30	794.75	0	539.55	112.8	27.93	900	10.5	2385.53
B5/H10	748	1.375	539.55	112.8	35.91	720	3.5	2161.135
B5/H20	748	1.375	539.55	112.8	31.92	900	7	2340.645
B5/H30	748	1.375	539.55	112.8	27.93	1020	10.5	2460.155
B10/H10	701.25	2.75	539.55	112.8	35.91	768	3.5	2163.76
B10/H20	701.25	2.75	539.55	112.8	31.92	900	7	2295.27
B10/H30	701.25	2.75	539.55	112.8	27.93	1080	10.5	2474.78
B15/H10	654.5	4.125	539.55	112.8	35.91	780	3.5	2130.385
B15/H20	654.5	4.125	539.55	112.8	31.92	960	7	2309.895
B15/H30	654.5	4.125	539.55	112.8	27.93	1140	10.5	2489.405
B20/H10	606.9	5.5	539.55	112.8	35.91	840	3.5	2144.16
B20/H20	606.9	5.5	539.55	112.8	31.92	1008	7	2311.67
B20/H30	606.9	5.5	539.55	112.8	27.93	1176	10.5	2479.18
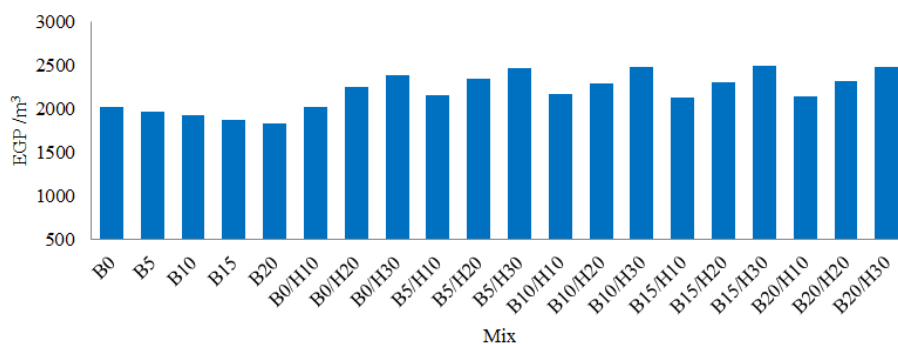
Figure 13. cost per concrete cubic meter of all studied mixes

7. Conclusions

The concluding remarks can be summarized as follows:

1. Incorporating BS as a partial cement replacement decreases fresh properties. Inclusion for HM required high dosages of chemical admixture to achieve and maintain SCC requirements.

2. Compressive strength at the age of 90 days was improved by 8% due to incorporating 5% BS as an optimum cement replacement ratio.

3. Inclusion of HM as a partial sand replacement significantly improves compressive strength with an increasing replacement ratio up to 30%.

4. Maximum improved compressive strength reached 16.5% higher than control mix (without waste powders) by incorporating 5%BS as cement replacement with 30% HM as sand replacement (mix B5/H30), this is valid for the age of 90 days.

5. Sorptivity decreased by about 12.38, 24.5 and 26% while, UPV increased by 9, 13 and 17% for mixes containing 5%BS, 30%HM and (5%BS+30%HM) respectively. This is explained by the reduction in porosity as confirmed by microstructure studies; this is valid for mixes tested at the age of 28 days.

6. The use of 15% silica fume together with waste powders (B5/H30) in ternary blended cements was found to have a superior influence on concrete behavior. SEM images for the control mix showed micro-cracks and increased porosity. In addition, thick, dense areas are free of porosity

7. Compressive strength values were increased due to exposure0 to elevated temperatures0 up0 to0 200°C. The percentage of increasing compressive strength was less than 3% for all mixes.

8. XRD showed that Quantification of the phases by Rietveld refinements reveals meaningful trends - samples B5, B0/H30 and B5/H30 show higher C-S0-H& higher portla0ndite percentages tha0n average, indicating faster cement hydration. The compositional details obtained on the key binding phases will help correlate composition-microstructure-property relationships in subsequent concrete performance studies.

9. The obtained enlarged pore surfac0e ar0ea in the modified concrete mixes (B5, B0/H30, and B5/H30) may reveal an intricate relationship between po0re si0ze and surfa0ce area, where the addition of supplementary materials may impose an additional barrier in smaller pores, effectively reducing their availability for adsorption. Hence, the observed raise in pore surfac0e are0a may not solely be contributed to an augmented porosity.

10. Incorporating both BS and HM may increase the cost of the mix while reducing embodied CO_2 compared to control mix and, hence, improve the environmental impact.

REFERENCES

[1] Darko, A.; Chan, A.P.; Owusu-Manu, D.-G.; Ameyaw, E.E.(2017). "Drivers for implementing green building technologies: An international survey of experts." J. Clean. Prod. Vol. 145, pp.386–394. [CrossRef]

[2] Dimitriou, G.; Savva, P.; Petrou, M.F. (2018) "Enhancing mechanical and durability properties of recycled aggregate concrete." Constr. Build. Mater. Vol. 158, pp.228–235. [CrossRef]

[3] Shen, W.; Wu, J.; Du, X.; Li, Z.; Wu, D.; Sun, J.; Wang, Z.; Huo, X.; Zhao, D. Cleaner .(2022)".production of high-quality manufactured sand and ecological utilization of recycled stone powder in concrete." J. Clean. Prod. Vol. 375, pp. 134146. [CrossRef]

[4] Tang .S.W., Yao .Y, Andrade .C, Andrade, Z.J. Li, (2015) "Recent durability studies on concrete structure", Cem. Concr. Res.

[5] P.K. Mehta, P.J.M. Monteiro,(2006) "Concrete: Microstructure, Properties and Materials", McGraw-Hill, New York,Vol. 3rd ed.

[6] Parvathy, C. Karthika, V. Gayathr,(2018) "Experimental studies on durability aspects of high strength concrete using flyash and alccofine", Int. J. Recent Technol. Eng. Vol.7 , pp.423–427.

[7] European Federation of National Associations, Aggregates for mortar, EN 13139 (2018).

[8] G. Moir, S. Kelham, (1997)"Developments in manufacture and use of Portland limestone cement, in: V.M. Malhotra (Ed.), Proceedings of High-Performance Concrete, ACI SP-172, American Concrete Institute, Detroit, MI, pp. 797– 819.

[9] H.M. Bustnes, B. Lagerblad, E. Forssberg,(2004) "The function of fillers in concrete", Mater. Struct. Vol.37, pp. 74–81.

[10] I. Soroka, N. Setter (1977) "The effect of fillers on strength of cement mortars", Cem. Concr. Res. 7 (4), pp. 449–456.

[11] I. Soroka, N. Stern, (1976)"Calcareous fillers and the compressive strength of Portland cement", Cem. Concr. Res. 6 (3) pp. 367–376.

[12] H. Moosberg, B. Lagerblad, E. Forssberg, (2004)" The function of fillers in concrete", Mater. Struct. Vol.37, pp. 74–81.

[13] J.J. Thomas, H.M. Jennings, J.J. Chen,(2009)" Influence of nucleation seeding on the hydration mechanisms of tricalcium silicate and cement", J. Phys. Chem. Vol.113 (11), pp.4327–4334.

[14] M. Hubler, H. Jennings, J. Thomas, (1976)"Influence of nucleation seeding on the compressive strength of ordinary portland cement and alkali activated blast furnace slag", Infrastructure Technology Institute Year 2 Final Report, Northwestern University.

[15] K.E. Alyamac et al. (2017) " Development of eco-efficient self-compacting concrete with waste marble powder using the response surface method "J. Clean. Prod.

[16] T. Ramos et al. (2013) " Granitic quarry sludge waste in mortar: Effect on strength and durability" Constr. Build. Mater.

[17] A. Rana et al. (2015) " Sustainable use of marble slurry in concrete" J. Clean. Prod.

[18] M. Tennich et al.)2017) " Behavior of self-compacting concrete made with marble and tile wastes exposed to external sulfate attack " Constr. Build.Mater .

[19] R.A. Schankoski et al.(2019) , "Fresh and hardened properties of self-compacting concretes produced with diabase and gneiss quarry by-product powders as alternative fillers " Constr. Build. Mater.

[20] A. Lozano-Lunar et al.(2020) "Performance of self-compacting mortars with granite sludge as aggregate" Constr. Build. Mater.

[21] G. Rojo-López et al.(2020)" Quaternary blends of portland cement, metakaolin, biomass ash and granite powder for production of self-compacting concrete" J. Clean Prod.

[22] E. Elyamany a, Abd Elmoaty M. Abd Elmoaty a, Basma Mohamed b (2014) "Effect of filler types on physical, mechanical and microstructure of self compacting concrete and Flow-able concrete" Alexandria Engineering Journal,Vol. 53, Issue 2, pp 295-307.

[23] Vijayalakshmi, M., Sekar, A.S.S., Ganesh prabhu, G. (2013) "Strength and Durability Properties of Concrete Made with Granite Industry Waste". Constr. Build. Mater, Vol.46,pp 1–7. [CrossRef]

[24] M, Dobiszewska a, et al, (2023) "Utilization of rock dust as cement replacement in cement composites: An alternative approach to sustainable mortar and concrete productions" Journal of Building Engineering, vol. 69, 106180.

[25] Bentz D. P., Ehlen M. A., Ferraris C. F., and Winpigler J. A.,(2001), "Service Life Prediction Based on Sorptivity for Highway Concrete Exposed to Sulfate Attack and Freeze-Thaw Conditions," FHWA-RD-01-162.

[26] European Federation of National Associations Representing producers and applicators of specialist building products for Concrete (EFNARC), 2002 "Specification and guideline for self- compacting concrete".p.32

[27] S.S. Vivek, G. Dhinakaran, (2017) " Fresh and hardened properties of binary blend high strength self-compacting concrete", Eng. Sci. Technol. Int. J. pp.1173– 1179, https://doi.org/10.1016/j.jestch.2017.05.003.

[28] M. Nehdi, M. Pardhan, S. Koshowski, (2004)" Durability of self-consolidating concrete incorporating high-volume replacement composite cements", Cem. Concr. Res. ,Vol.34,pp. 2103–2112, https://doi.org/10.1016/j.cemconres.2004.03.018.

[29] Rakesh Choudhary, Rajesh Gupta, Ravindra Nagar, (2020)" Impact on fresh, mechanical, and microstructural properties of high strength self-compacting concrete by marble cutting slurry waste, fly ash, and silica fume" Constr. Build. Mater. Vol. 239, 117888.

[30] A. Khodabakhshian, M. Ghalehnovi, J.D. Brito, E.A. Shamsabadi, (2018)" Durability performance of structural concrete containing silica fume and marble industry waste powder", J. Cleaner Prod.

[31] Magdalena Dobiszewska, and Ahmet Beycioglu , (2020)," Physical Properties and Microstructure of Concrete with Waste Basalt Powder Addition " Materials Journal, 13 (16), 3503; https://doi.org/10.3390/ma13163503.

[32] Kurdowski,W.(2014) "Cement and Concrete Chemistry"; Springer: Dordrecht, The Netherlands.

[33] Vijayalakshmi, M.; Sekar, A.S.S.; Ganesh prabhu, G. (2013) "Strength and Durability Properties of Concrete Made with Granite Industry Waste." Constr. Build. Mater. Vol.46,pp 1–7.

[34] Singh, S.P. Singh,(2018) "Evaluating the performance of self-compacting concretes made with recycled coarse and fine aggregates using non-destructive testing techniques", Constr. Build. Mater. Vol.181 ,pp.73–84.

[35] Behnood A., Ziari H. (2008) "Effects of silica fume addition and water to cement ratio on the properties of high-strength concrete after exposure to high temperatures" Cem. Concr. Compos. Vol. 30, pp.106–112.

[36] Hammond, G.P., Jones, C.I., (2008)." Embodied energy and carbon in construction materials". Proc. Inst. Civ. Eng. Energy

[37] Chiaia, B., Fantilli, A.P., Guerini, A., Volpatti, G., Zampini, D., (2014). "Eco-mechanical index for structural concrete". Constr. Build. Mater. Vol 67, Part C, pp. 386-392.

[38] Reiner, M., 2007. "Technology, Environment, Resource and Policy Assessment of Sustainable Concrete in Urban Infrastructure". Diss. U of Colorado at Denver.